An Algorithm for Multisource Beamforming and Multitarget Tracking

Sofiène Affes, Saeed Gazor, and Yves Grenier, *Member, IEEE*

Abstract— **A new algorithm for simultaneous robust multisource beamforming and adaptive multitarget tracking is proposed. Self-robustness to locations errors or variations is introduced by a source-subspace-based tracking procedure of steering vectors in the array manifold. This LMS-type procedure is generalized from a former work we developed in the single source case. Two beamforming structures are actually proposed. The first is adaptive and optimal for uncorrelated sources and correlated noise. The second is conventional and optimal for correlated sources and uncorrelated white noise. The proposed algorithm and MUSIC show an identical asymptotic variance in localization for immobile sources, whereas for the mobile case, the proposed algorithm is highly advantageous. Then, it is shown that the additional use of some kinematic parameters (i.e., speed, acceleration, etc.) inferred from the reconstructed trajectories improves the tracking performance and overcomes some of the problems of crossing targets. The efficiency of multitarget tracking and the robustness of multisource beamforming are proved and then confirmed by simulation. The number of sources can be initialized and tracked by a marginal proposed procedure. The beamforming performance is shown to be optimal as the single source case. Finally, the algorithm has a very low order of arithmetic complexity.**

I. Introduction

RECENTLY, we proposed in [1]–[3] a robust adaptive beamformer based on a LMS-type subspace algorithm for the tracking of a single source by allowing the steering vector of a classical beamformer to be time adapted in the array manifold. This algorithm proved to be self-robust to strong localization errors without introducing any signal-to-noise ratio (SNR= $\frac{\sigma_s^2}{\sigma_N^2}$) loss and to have an efficient tracking behavior when in the presence of mobile sources (target and jammers). This concept of self-robustness with adjusted robust adaptive beamforming is explained in more detail in [1]–[3].

In this paper, our purpose is to generalize this algorithm to the simultaneous extraction and tracking of multiple desired sources [4]. To do so, we particularly assume that the number and the location parameters of desired point sources, among all present sources including jammers, are initialized by an approximate localization technique or simply given with errors. Those jammers not localized will have relatively small power and will be confused with noise.

Manuscript received February 6, 1995; revised September 14, 1995. The associate editor coordinating the review of this paper and approving it for publication was Roger S. Cheng.

S. Affes is with the Institut National de la Recherche Scientifique—Télécommunications, Ile des Soeurs, Verdun H3E 1H6 Canada (e-mail: affes@inrs-telecom.uquebec.ca).

S. Gazor and Y. Grenier are with the Ecole Nationale Supérieure des Télécommunications, Département Signal, 75634 Paris Cedex 13, France.

Publisher Item Identifier S 1053-587X(96)03965-7.

Localization methods may be used in the case of a stationary environment to reliably estimate the correct source positions and the corresponding steering vectors. However, they use a time average for the estimation of the covariance matrix that does not yield an adequate estimator when in the presence of fast moving targets (i.e., nonergodic observations). Consequently, the performance of such techniques drastically deteriorates. Several estimation techniques such as Kalman filtering have been combined with localization algorithms and applied in target motion analysis to estimate the trajectory of an object [6]–[11]. However, all these methods are expensive in terms of computational complexity. Another class of techniques propose adaptive or batch implementations of these algorithms by subspace-based tracking procedures (e.g., [17] and [18]). With m sensors, the computationally efficient methods of subspace tracking require at least $O(mp)$ operations for every update where p is the number of all present sources without the location parameter search, whereas the proposed algorithm requires only $O(mp)$ operations, including localization, where p denotes the number of desired sources among all present sources. In addition, unlike most of these techniques, it does not require the knowledge of the noise covariance matrix nor the number of all present sources.

The simulations confirm the results we expected from the generalization of the convergence and performance analyzes. Indeed, the algorithm has the same robustness regarding location errors. However, two problems that were expected theoretically are encountered. First, the location estimator is biased whenever the location parameter increment is not zero mean (e.g., in the presence of maneuvering targets). Second, the algorithm cannot deal with crossing targets, as the presence of a unique source in the spread of a locking range is a major hypothesis for the convergence proof in [1]–[3]. We thus introduce an additional procedure based on the use of some kinematic parameters such as the speed. It is shown that this procedure removes the bias and overcomes some of the problems of crossing targets by prediction of crossover points on trajectories and by blocking the tracking procedure during crossover intervals.

After making a mathematical formulation in Section II, we present the different steps of the algorithm in Section III. Actually, the proposed algorithm in a first version fails in tracking the crossing sources. This problem is addressed in Section III-D, where an efficient solution is given. We briefly address both the detection and initialization of a newly appeared source and the detection of a vanishing source as a marginal proposition in Section III-E. In Section IV, we

make convergence and performance analyzes and show that the algorithm has a better tracking/localization behavior than the asymptotic behavior of MUSIC [18], [19] even for immobile sources (see [1] and [3]). The simulation results are presented in Section V. In Section VI, we shall draw our conclusions.

II. Mathematical Formulation

We consider the following model of signals received by a linear array

$$\begin{aligned} X_t &= G_t S_t + N_t \\ G_t &= [F(\kappa_{1,t}), F(\kappa_{2,t}), \cdots, F(\kappa_{p,t})] \end{aligned} \tag{1}$$

where X_t is the m-dimensional observation vector, $S_t = [s_{1,t}, s_{2,t}, \cdots, s_{p,t}]^T$ is the vector of p desired narrowband signals to be extracted ($p \leq m$) among all present sources, N_t is an additive noise vector, and G_t is the transfer function (i.e., the $m \times p$ steering matrix) between the emitted sources S_t and the m-sensor antenna array. All the quantities considered herein are complex. F is a parametric modeling function determining the propagation law and the configuration geometry, and $\Theta_t = [\kappa_{1,t}, \kappa_{2,t}, \cdots, \kappa_{p,t}]^T$ is the location parameter of interest. $\kappa_{i,t}$ represents the DOA or the spatial coordinates of the source $s_{i,t}$. The subscript t stands for time index.

We consider here the case of a plane-wave propagation model and a linear array, for the sake of simplicity, though a 2-D or a 3-D array could be considered in general (e.g., see [24] for a 2-D array). Consequently, the parameterizing function F is given by

$$F(\kappa) = \left[e^{-j\kappa x_1}, e^{-j\kappa x_2}, \cdots, e^{-j\kappa x_m}\right]^T \tag{2}$$

where the wavenumber $\kappa \triangleq \frac{2\pi \sin(\phi)}{\lambda}$ represents a single source location parameter. $\phi \in [-\pi/2, \pi/2]$ is the DOA, and λ is the wavelength. The array center is considered to be at the origin (i.e., $\sum_{i=1}^{m} x_i = 0$, where $[x_1, x_2, \cdots, x_m]^T$ is the sensor positions vector; see [1]–[3] for more details). We make the following further assumptions:

- A1: G, N, and S are mutually independent.
- A2: Channel G is slowly time varying in comparison with the variations of N and S. Hence, we are able to properly estimate G and then update it.
- A3: The number of desired sources is initially known and a possibly erroneous approximation of Θ_0, say $\hat{\Theta}_0$, is initially provided either by an approximate *a priori* guess or by a given localization technique.
- A4: The DOA's are far enough apart to make the source separation possible. The validity of this assumption is tested continuously in a second version of the algorithm. Whenever it is invalid, we will use an alternative procedure presented in Section III-D.

In A1, source signals in S can be mutually correlated, whereas no particular assumption is made over the spatial structure of noise. In A3, it should be noted that p does not necessarily denote the number of all present sources.

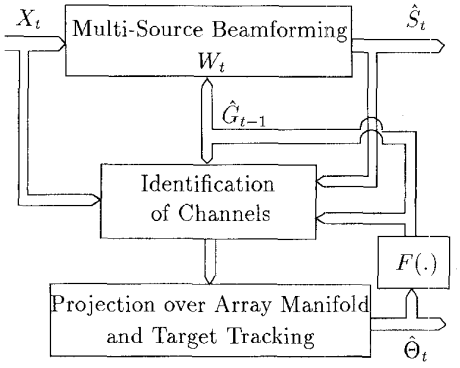

Fig. 1. Structure of the multi-source algorithm in three steps: Beamforming, identification of channels, and projection over the array manifold and target tracking.

III. Proposed Algorithm

Given these assumptions, the main purpose in this paper is to constantly correct the estimated wavenumbers and time adapt the beamformers to the new look directions. The algorithm should thus provide a robust multisource beamforming, and an efficient method for multitarget tracking. The LMS-type algorithm can be summed up by the steps presented in the following sections, as shown in Fig. 1.

A. Multisource Beamforming

The adaptive beamformer proposed in [1]–[3] could be successfully used in parallel to track each selected desired source and to adaptively cancel all the present jammers (possibly including those unlocalized sources) when in the presence of no coherent source interference and spatially correlated noise. The idea is to simultaneously time adapt all the steering vectors in the same way as in [1]–[3] with a separate projection of each vector on the array manifold.

Instead of several adaptive beamformers in parallel, a set of conventional beamformers could be used that have an optimal performance in the presence of uncorrelated white noise. Although the unlocalized sources are not specifically cancelled, the performance remains barely unchanged since we assumed these sources to be confused with noise. In this case, p necessarily denotes the number of all localized sources. The advantage of these beamformers of being nonadaptive is that they avoid source signal cancelation, even in the presence of partially coherent interference.

At iteration t, we suppose that an estimation of G_{t-1}, say $\hat{G}_{t-1}$, is available from the previous iteration or initialized by $\hat{G}_0 = F(\hat{\Theta}_0)$. As assumption A2 states that G is slowly time varying, it is possible to estimate S_t with the steering matrix G_t approximated by $\hat{G}_{t-1}$ at time t. In the following, we first present an adaptive beamformer with a GSC structure based on a LMS algorithm as a generalization of the proposed algorithm in [1]. Afterwards, in Section III-A2), we propose the use of conventional beamforming instead.

1) Adaptive Beamformers with GSC Structure: For the estimation of $s_{i,t}$ with $\hat{G}_{i,t-1}$ as the steering vector, adaptive beamformers could be used as in [1] to adaptively cancel the other emitted sources (possibly unlocalized) with optimal

reduction of correlated noise. For each desired source $1 \leq i \leq p$, we consider an adaptive beamformer with a GSC structure [5] based on the LMS algorithm [22] as follows:

$$\begin{aligned} X_{i,t}^s &= \text{diag}[\hat{G}_{i,t-1}^H] X_t \triangleq [X_{1,i,t}^s, \cdots, X_{m,i,t}^s]^T \\ y_{i,t} &= \frac{1}{m} \sum_{l=1}^{m} X_{l,i,t}^s \\ X_{i,t}^n &\triangleq [X_{1,i,t}^s, X_{2,i,t}^s, \cdots, X_{m-1,i,t}^s]^T - y_{i,t} \mathbf{1}_{m-1} \\ \hat{s}_{i,t} &= y_{i,t} - W_{i,t}^{n\,H} X_{i,t}^n \\ W_{i,t+1}^n &= W_{i,t}^n - \eta_{i,t} \hat{s}_{i,t}^H X_{i,t}^n. \end{aligned} \tag{3}$$

U^H denotes the conjugate transpose of U, and $W_{i,t}^n$ and $\mathbf{1}_{m-1} \triangleq [1, 1, \cdots, 1]^T$ are two $(m-1)$-dimensional vectors. We note that $W_{i,t}^n$ is initially set to 0. The step-size of the GSC $\eta_{i,t}$ could be constant (i.e., $\eta_{i,t} \triangleq \eta_0$ for LMS-GSC) or could include a normalization factor (e.g., $\eta_{i,t} \triangleq \eta_0 / ||X_{i,t}^n||^2$ for NLMS-GSC) to improve the convergence behavior of the array in the presence of fast-moving jammers. The estimated signal vector $\hat{S}_t \triangleq [\hat{s}_{1,t}, \hat{s}_{2,t}, \cdots, \hat{s}_{p,t}]^T$ will be used later in the estimation of steering vectors and source locations.

2) Conventional Beamforming: It is shown in [2] and [3] that conventional beamformers defined by

$$\hat{S}_t = W_t^H X_t \triangleq \left(\hat{G}_{t-1}^H \hat{G}_{t-1}\right)^{-1} \hat{G}_{t-1}^H X_t \tag{4}$$

are optimal for the minimization of the output distortion in the presence of localized sources (possibly mobile with partially coherent interference) and spatially white noise. W_t in (4) denotes the $m \times p$ beamforming matrix and is used instead of (3). It must be noted that under the assumption A4, the matrix G_t is full column rank and that $\hat{G}_t^H \hat{G}_t$ is invertible. Moreover, the "nonmixture and distortion-less constraint" $W_t^H \hat{G}_{t-1} = I_p$ is fulfilled (see [1]–[3]). Hence, for each one of the p sources, say $s_{i,t}$, the corresponding column beamformer $W_{i,t}$ (i.e., $W_t = [W_{1,t}, \cdots, W_{p,t}]$) considers the remaining sources $s_{j,t}$ $(j \neq i)$ as jammers and rejects them.

Unlike adaptive beamformers for a given $\hat{G}_{t-1}$, the performance of signal separation in (4) is not affected by the coherence between two sources $s_{i,t}$ and $s_{j,t}$ $(j \neq i)$. Moreover, it shows a better performance than the GSC beamformers in the presence of fast mobile targets. However, the arithmetic complexity in flops of the conventional beamforming and GSC are, respectively, equal to $mp^2 + mp + p^3 + p^2$ and $4mp$. In addition, unlike adaptive beamformers, conventional beamforming is not optimal for the reduction of spatially correlated noise.

When the output SNR is high, a modification in (4) could be introduced to further reduce the arithmetic complexity to $m(p+1)$ at the expense of an output SNR loss as follows:

$$\hat{S}_t \triangleq \hat{G}_{t-1}^H \Omega X_t \tag{5}$$

where Ω is a diagonal matrix representing a weighting window such as Kaiser's with an improved mainlobe to sidelobe ratio [23]. A well-selected window could also improve the locking range of the algorithm and reduce the sidelobe effects. We point out that unlike (3) and (4), the beamformer in (5) cannot efficiently remove the interference of possibly present jammers in the mainlobe of the array. Further results regarding complexity reduction and the general case of optimal coherent source extraction in correlated noise were recently given in [3].

B. Channel Identification

The resulting estimate of S_t obtained by one of the above methods (3)–(5), say $\hat{S}_t$, can be used in a LMS-type procedure to track or identify the steering matrix variations by

$$\tilde{G}_t = \hat{G}_{t-1} + (X_t - \hat{G}_{t-1} \hat{S}_t)(\mu \hat{S}_t)^H \tag{6}$$

where $\tilde{G}_t \triangleq [\tilde{G}_{1,t}, \tilde{G}_{2,t}, \cdots, \tilde{G}_{p,t}]$. It should be noted at this stage that the column vectors $\tilde{G}_{i,t}$ do not necessarily belong to the array manifold. For this reason, we denote them, at present, by $\tilde{G}_t$ in (6). The step size μ is a scalar but could be, in general, a diagonal matrix for regulating the time constants of the sources separately. Equation (6), combined with a multisource beamformer (presented in the previous subsection), represents a source subspace tracking algorithm (see [1]–[3]) similar to the procedure given by Yang [17]. In the single source case, it is similar to the algorithm proposed by Oja [6]. We note that (6) can be interpreted as the result of a LMS procedure obtained by the minimization of the energy of the observed signals after projection on the noise subspace orthogonal to $\hat{G}_{t-1}$. More details can be found in [1]–[3].

The convergence analysis and simulations show that (6) does not correctly track the steering vectors when assumption A4 is not fulfilled. This is actually due to the fact that the noise covariance matrix defined for one selected source can no longer be approximated by the "nice" form $\sigma_N^2 I$ when one or more sources are present in its locking range (see [1]–[3]). To overcome this problem, we will introduce a new procedure presented later in Section III-D.

C. DOA Estimation and Source Tracking

At present, we consider that assumption A4 is valid. In this case, the estimator $\tilde{G}_{i,t}$ of $G_{i,t}$ (ith column of G_t) can be improved by a DOA adjustment with respect to a projection over the array manifold, performed separately for each source as in [1]–[3]. The ith location parameter $\hat{\kappa}_{i,t}$ is then updated as follows for $1 \leq i \leq p$:

$$\hat{\kappa}_{i,t} = \hat{\kappa}_{i,t-1} - \frac{\sum_{q=1}^{m} x_q \text{Im}\{\log(\tilde{G}_{q,i,t} e^{j x_q \hat{\kappa}_{i,t-1}})\}}{\sum_{q=1}^{m} x_q^2} \tag{7}$$

where $\tilde{G}_{q,i,t}$ is the qth component of the ith column vector $\tilde{G}_{i,t}$ of the matrix $\tilde{G}_t$ at time t, and where $\text{Im}\{\cdot\}$ denotes the imaginary part of a complex number. It must be noted that another alternative is also presented in [4] instead of (7). Hence, we finally reconstruct the steering matrix

$$\hat{G}_t \triangleq [F(\hat{\kappa}_{1,t}), F(\hat{\kappa}_{2,t}), \cdots, F(\hat{\kappa}_{p,t})]. \tag{8}$$

D. Speed Estimation and Tracking of Crossing Targets

We notice that the above algorithm gives unbiased location estimators, unless the location increments are not zero mean (see (17)). Hence, in this section, we present an additional step in the algorithm to improve its performance regarding the bias

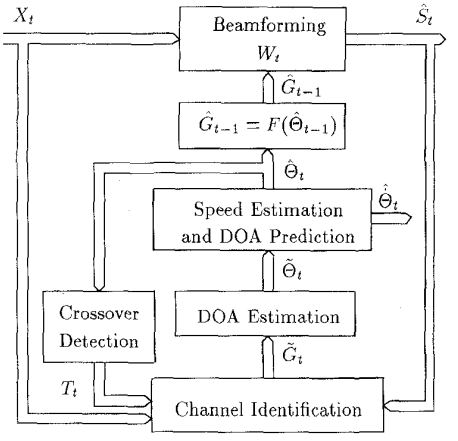

Fig. 2. Block diagram of the algorithm with speed estimation and crossover detection.

of the location parameters and to avoid some of the problems of crossing targets. This step is based on the prediction of the target trajectories thanks to the extra information obtained on their kinematics. Park *et al.* [14] modified a multiple target angle tracking algorithm presented by Sword *et al.* [12]. They showed that the use of predicted angles and the estimation of the target speeds improve the tracking performance of the algorithm for crossing targets. Rao *et al.* [11] proposed an algorithm to set up a correspondence between estimates and targets by the prediction of future positions based on previous trajectories. These algorithms, like ours, have the attractive feature of simple structure and avoid data association problems. In accord with the literature of target motion analysis [6]–[9], [14], we use the estimated kinematic parameters to rule the behavior of the targets during the crossover interval, whereas outside this interval, we propose the use of these parameters to remove the bias of the location estimators as shown in Fig. 2.

Let us assume the speed or the target motion increment of the ith source noted by $\dot{\kappa}_{i,t} \triangleq \kappa_{i,t+1} - \kappa_{i,t}$ to be slowly time varying. We are then able to estimate the speeds for $1 \leq i \leq p$ by replacing (7) by the following procedure:

$$\tilde{\kappa}_{i,t} = \hat{\kappa}_{i,t-1} - \frac{\sum_{q=1}^{m} x_q \mathrm{Im}\{\log(\tilde{G}_{q,i,t} e^{jx_q \hat{\kappa}_{i,t-1}})\}}{\sum_{q=1}^{m} x_q^2} \quad (9)$$

$$\hat{\dot{\kappa}}_{i,t} = (1-\alpha)\hat{\dot{\kappa}}_{i,t-1} + \alpha(\tilde{\kappa}_{i,t} - \tilde{\kappa}_{i,t-1}) \quad (10)$$

$$\hat{\kappa}_{i,t} = \tilde{\kappa}_{i,t} + \hat{\dot{\kappa}}_{i,t} \quad (11)$$

where $\hat{\dot{\kappa}}_{i,0} = 0$. The speed is estimated in (10) via a smooth lowpass AR filtering of an intermediate location estimator $\tilde{\kappa}_{i,t}$ with a smoothing factor $0 \leq \alpha \leq 1$. This factor must be chosen with respect to the stationarity and the bandwidth of $\dot{\Theta}_t$ and the time constants of the algorithm.

It can be seen that the intermediate location estimator in (9) as in (7) tracks the targets with a delay equal to the product of the speed by the corresponding time constant. For trajectories with slowly time-varying increments, this delay is negligible, and, therefore, $(\tilde{\kappa}_{i,t} - \tilde{\kappa}_{i,t-1})$ could be considered to be an estimator of the target speed $\dot{\kappa}_{i,t}$. Hence, the final location estimator in (11) catches up with the bias due to the target speeds at convergence under some stability conditions on α and μ. Details are given in Section IV.

However, when two targets are not distant enough (when they are in the same locking range), the source separation is no longer possible. Consequently, the algorithm fails to track them properly. For each source, we therefore define the following test of validity of assumption A4:

$$T_{i,t} \triangleq \begin{cases} 0, & \text{if} \exists j \neq i \text{ s.t. } |\hat{\kappa}_{i,t-1} - \hat{\kappa}_{j,t-1}| \leq \epsilon \\ 1, & \text{otherwise} \end{cases}$$

$$T_t \triangleq [T_{1,t}, T_{2,t}, \cdots, T_{p,t}]^T. \quad (12)$$

We note that $T_{i,t}$ is initially set to one. The value of ϵ should be chosen with respect to the array resolution. If this assumption is not valid, the adaptation of the channel identification based on the estimated signals in (6) should be blocked for the corresponding crossing targets. Hence, we modify it as follows:

$$\tilde{G}_t = \hat{G}_{t-1} + (X_t - \hat{G}_{t-1}\hat{S}_t)(\mu \ \mathrm{diag}[T_t]\hat{S}_t)^H. \quad (13)$$

We are now able to keep tracking crossing trajectories, even during the crossover intervals, where we can see that the speed estimates remain constant. This is actually a good and reasonable approximation for targets locally crossing with uniform speed. In the case where the motion of the targets is more complex (e.g., uniformly accelerated trajectories, etc.), we may estimate higher order increments by an alternative procedure as shown in [2] and [3] (i.e., acceleration, third derivative, etc.). It should be noted that the estimation and the use of higher order increments do not significantly improve the precision of the source localization, but they do enable a better prediction of the target trajectory during the crossover interval (see Fig. 8). These additional steps could improve the target tracking performance in real situations and do not introduce a high order of computational complexity.

The global algorithm can be summed up by the following steps (see Fig. 2):

- First, one of (3), (4), or (5) is used for beamforming.
- Equation (12) predicts local crossover points.
- Then, (13) identifies the steering vectors.
- The results are followed by the speed and position estimation procedure in (9)–(11).
- Finally, to close the tracking loop, the steering matrix updated by (8) will be feedbacked in the beamforming unit for the next iteration.

E. Source Number Tracking

This section proposes two marginal procedures for adaptively detecting the number of sources p when additive noise is almost white and uncorrelated. By the results of these procedures, the dimension of the steering matrix should be properly modified if necessary. More elaborate methods for estimating the number of sources do exist (e.g., in [20] and [21]).

1) Presence Verification of the Tracked Sources: Let us define $\hat{N}_t = (X_t - \hat{G}_{t-1}\hat{S}_t)$. The presence of each tracked source could be verified by an energy detection criterion. To do so, we

may estimate the energy of the emitted sources for $1 \leq i \leq p$ by a simple recursive algorithm

$$e_{i,t} = (1-a)e_{i,t-1} + a\left(|\hat{s}_{i,t}|^2 - \frac{\|\hat{N}_t\|^2}{m^2}\right) \tag{14}$$

where $0 < a < 1$ is a smoothing factor. If the ith source is well localized, $e_{i,t}$ represents a time-smoothed estimator of its signal input power. On the other hand, in the absence of the ith source, $e_{i,t}$ should be close to zero in average. Hence, the detection could be made by comparing $e_{i,t}$ with a well defined threshold.

2) Detection and Initialization of a New Appearing Source: We may apply a simple adaptive tracking procedure to identify the eigenvector corresponding to the highest eigenvalue of $E[\hat{N}_t\hat{N}_t^H]$ (e.g., [15] and [17]). In particular, we propose the procedure of Oja [16]

$$\begin{cases} \tilde{y}_t = \frac{\tilde{G}_{p+1,t-1}^H \hat{N}_t}{m} \\ \tilde{G}_{p+1,t} = \tilde{G}_{p+1,t-1} + \mu_d(\hat{N}_t - \tilde{G}_{p+1,t-1}\tilde{y}_t)\tilde{y}_t^H. \end{cases} \tag{15}$$

When an unlocalized source appears, $\tilde{G}_{p+1,t}$ converges to a new steering vector, and after the convergence, $\tilde{y}_t$ is an estimate of the new source signal. Hence, we may estimate the energy of a potential source by the following equation:

$$e_{p+1,t} = (1-a)e_{p+1,t-1} + a\left(|\tilde{y}_t|^2 - \frac{\|\hat{Z}_t\|^2}{m(m-1)}\right) \tag{16}$$

where $\hat{Z}_t = \hat{N}_t - \tilde{G}_{p+1,t-1}\tilde{y}_t$. Finally, the detection could be made as above by comparing $e_{p+1,t}$ with a well-defined threshold. We note that although $\tilde{G}_{p+1,t}$ is considered to be an initialization for the nonprojected steering vector on the array manifold for a new detected source, the recursive DOA estimation in (7) could not be applied immediately. In this case and only in the first iteration after the detection of a new source, $\hat{\kappa}_{p+1,t-1}$ could be initialized by a search minimization of $\|\tilde{G}_{p+1,t} - F(\kappa)\|$ over m uniformly distributed points in the range of κ.

IV. Convergence and Performance Analyses

In this section, we consider here the convergence of localization errors. The performance analysis of the proposed algorithm for incoherent sources and $\alpha = 0$ shows for the ith source ($1 \leq i \leq p$) that (see [2] and [3])

$$E[\hat{\kappa}_{i,t}] = E[\hat{\kappa}_{i,t-1}]\left(1 - \mu\sigma_{s_i}^2\right) + \mu\sigma_{s_i}^2 E[\kappa_{i,t}] \tag{17}$$

where $\sigma_{s_i}^2$ is the variance of $s_{i,t}$. This equation proves that the algorithm is able to track each target in the temporal mean with a time constant given by $\tau_{E[\hat{\kappa}]} = \frac{1}{\mu\sigma_s^2}$. To show the efficiency of this algorithm, we compare it with the well-known algorithm of MUSIC for DOA estimation for an immobile single source. In [1]–[3], for $\alpha = 0$, it was shown (when μ is small) that this algorithm converges in covariance with a time constant equal to $\tau_{\mathrm{Cov}(\hat{\kappa})} = \frac{1}{2\mu\sigma_s^2}$ and a misadjustment of the localization error (i.e., the steady-state covariance of $\hat{\kappa}$) equal to

$$\mathrm{Cov}(\hat{\kappa}_\infty) = \frac{\mu\sigma_N^2\left(1 + \frac{1}{m(\mathrm{SNR})}\right)}{4\sum_{i=1}^m x_i^2}, \quad \alpha = 0 \tag{18}$$

From [18] and [19], we observe that the asymptotic variance of the DOA estimate is given for MUSIC by

$$\mathrm{Cov}_{\mathrm{MUSIC}}(\hat{\kappa}_{T_s}) = \frac{\sigma_N^2\left(1 + \frac{1}{m(\mathrm{SNR})}\right)}{2T_s\sigma_s^2\sum_{i=1}^m x_i^2} \tag{19}$$

where $T_s \gg 1$ is the number of snapshots. We clearly see from (18) and (19) that the asymptotic variances of the DOA estimates given by MUSIC and the proposed algorithm are equal when the number of snapshots is equal to $T_s = 4\tau_{\mathrm{Cov}(\hat{\kappa})}$, the time in which initial errors are reduced up to 1.83% (see the simulations in [1]).

Let us now consider the case where $\alpha \neq 0$, and define the following state vector for the estimated localization error of each target by

$$\psi_{i,t} \triangleq \begin{bmatrix} \Delta\tilde{\kappa}_{i,t} \\ \Delta\hat{\kappa}_{i,t} \end{bmatrix} = \begin{bmatrix} \tilde{\kappa}_{i,t} - \kappa_{i,t} \\ \hat{\kappa}_{i,t} - \dot{\kappa}_{i,t+1} \end{bmatrix} \tag{20}$$

and $\Delta\hat{\kappa}_{i,t} \triangleq \hat{\kappa}_{i,t} - \kappa_{i,t+1}$. It has been shown in [1]–[3] that a necessary condition for convergence is that the localization errors $|\Delta\tilde{\kappa}_{i,t}|$ must be smaller than the mainlobe width of the array patterns. Under such a condition, we obtain in Appendix A for $1 \leq i \leq p$

$$\psi_{i,t} = \begin{bmatrix} 1 - r_{i,t} & 1 - r_{i,t} \\ -\alpha r_{i,t} & 1 - \alpha r_{i,t} \end{bmatrix}\psi_{i,t-1} + \begin{bmatrix} u_{i,t} \\ \alpha u_{i,t} + \ddot{\kappa}_{i,t} \end{bmatrix} \tag{21}$$

where $r_{i,t}$ and $u_{i,t}$ are given in Appendix A. The angular accelerations of the targets $\ddot{\kappa}_{i,t} \triangleq 2\kappa_{i,t} - \kappa_{i,t-1} - \kappa_{i,t+1}$ and $u_{i,t}$ are the inputs of these systems for $1 \leq i \leq p$. N_t and $s_{i,t}$ have zero mean as assumed in [2] and [3] for the need of analysis and are mutually independent from $\psi_{i,t-1}$. Thus, it is clear that $E[r_{i,t}\psi_{i,t-1}] = E[r_{i,t}]E[\psi_{i,t-1}] = \mu\sigma_{s_i}^2 E[\psi_{i,t-1}]$, and $E[u_{i,t}] = 0$. Hence, we have

$$E[\psi_{i,t}] = \mathbf{A}_i E[\psi_{i,t-1}] + \mathbf{B}_{i,t} \tag{22}$$

where $\mathbf{B}_{i,t} \triangleq [0, E[\ddot{\kappa}_{i,t}]]^T$, and

$$\mathbf{A}_i \triangleq \begin{bmatrix} 1 - \mu\sigma_{s_i}^2 & 1 - \mu\sigma_{s_i}^2 \\ -\mu\alpha\sigma_{s_i}^2 & 1 - \mu\alpha\sigma_{s_i}^2 \end{bmatrix}$$

is the transition matrix. The dynamics of these two-pole systems (22) are of time-invariant second-order lowpass AR filters with the mean angular accelerations at the input. Thus, they have adequate responses for the tracking of lowpass target trajectories.

Fig. 3 shows the eigenvalue positions of $\mathbf{A}_i$ for a given $\mu\sigma_{s_i}^2$ as a function of α on the complex plane. The stability condition implies that the eigenvalues of $\mathbf{A}_i$ have the absolute values smaller than one. Accordingly, we obtain the following condition for convergence in the mean:

$$0 < |1 - \mu\sigma_{s_i}^2| < 1 \Rightarrow 0 < \mu < \frac{2}{\sigma_{s_i}^2}. \tag{23}$$

Hence, under the stability condition and when the temporary mean of $\ddot{\kappa}_{i,t}$ is equal to zero, the mean of the state vector in

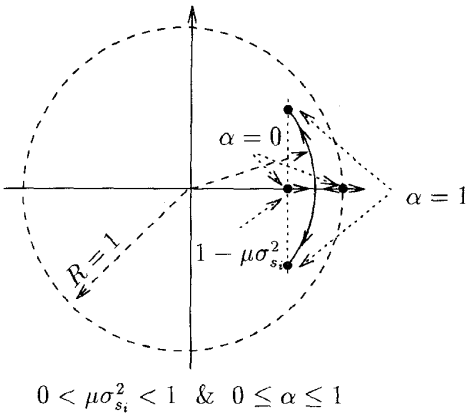

Fig. 3. Eigenvalue positions of $\mathbf{A}_i$ for $0 \leq \alpha \leq 1$ and a given $\mu\sigma_{s_i}^2 < 1$.

the steady state will converge to zero. The convergence of the mean state vector to zero shows that the algorithm is capable of tracking the target angles and their speeds. The time constants of the convergence are determined by the eigenvalues of $\mathbf{A}_i$ as functions of α and $\mu\sigma_{s_i}^2$. However, these time constants of $E[\tilde{\kappa}_{i,t}]$ are limited between $\frac{1}{\mu\sigma_{s_i}^2}$ and $\frac{2}{\mu\sigma_{s_i}^2}$ for $\alpha \in [0, 1]$.

Let us now define the covariance state vector by

$$\Psi_{i,t} \triangleq [E[|\Delta\tilde{\kappa}_{i,t}|^2], E[|\Delta\dot{\kappa}_{i,t}|^2], E[\Delta\tilde{\kappa}_{i,t}\Delta\dot{\kappa}_{i,t}]]^T. \quad (24)$$

In Appendix B, the iterative state (36) for the covariance of localization errors is derived by

$$\Psi_{i,t} = \Sigma_i \Psi_{i,t-1} + \Re_i$$

where the matrix Σ_i and the vector $\Re_i$ are, respectively, given by (37) and (38). The time constants and the stability of the algorithm are determined by the eigenvalues of the matrix Σ_i. For the ith source, the following results are obtained by numerical calculation with the theoretical expressions of Σ_i and $\Re_i$.

- The convergence condition obtained by the covariance analysis given by

$$0 < \mu < \mu_{\max} \triangleq \frac{1}{\sigma_{s_i}^2 + \frac{\sigma_N^2}{4m}}, \quad 0 \leq \alpha < 1 \quad (25)$$

  is stronger than (23) and is identical to [1]–[3] for $\alpha = 0$.
- Under this stability condition, for $0 < \alpha \leq \alpha_0(\mu)$ where $\alpha_0(\mu) = \frac{\mu\sigma_{s_i}^2}{2}[1 - \frac{\mu}{\mu_{\max}}]$, the time constants are almost equal to

$$\tau_{\text{Cov1}} \simeq \frac{1}{2\alpha}, \ \tau_{\text{Cov2}} \simeq \frac{1}{4\alpha_0(\mu) - 2\alpha}.$$

  In this case, τ_{Cov1} corresponds to the time constant of the speed estimation. For $\alpha_0(\mu) \leq \alpha < 1$, both time constants are almost equal to

$$\tau_{\text{Cov}} \simeq \frac{1}{2\alpha_0(\mu)}. \quad (26)$$

  This expression of $\tau_{E[\Delta\kappa^2]}$ shows the time constant of the algorithm to be infinitely large when the step size μ is very small or close to the stability bound $\mu_{\max}$ and lower bounded as a function of μ $\left(\text{i.e., } \tau_{\text{Cov}} \geq \frac{1}{m(\text{SNR})}\right)$. This bound improves with a higher SNR or sensor number m for a faster convergence.
- Equation (36) implies that the misadjustment of localization error (i.e., the steady-state covariance of $\Delta\tilde{\kappa}$) converges to the sum of two terms, respectively, resulting from the variations of noise and source position. The first term shows the intrinsic localization error for immobile targets due to noise perturbations. It shows the immediate effect of SNR, the number of sensors m, and sensor positioning x_i. The second term increases the localization error in κ for accelerating sources (maneuvering targets). It reduces with a smaller time constant and shows the effect of $\frac{\sigma_{\ddot{\kappa}}^2}{\sigma_s^2}$, where $\sigma_{\ddot{\kappa}}^2 = E[\ddot{\kappa}_t^2]$. Both terms show a compromise to be found over μ and α between a faster convergence rate and a smaller misadjustment of steady-state localization. As a function of μ and α, a lower bound for misadjustment can be found. This bound decreases with a higher SNR or smaller variations of source speed.

V. Simulation Results

In this section, we consider an equidistant linear array where the number of sensors is $m = 16$, and $x_{i+1} - x_i = 1$. We take $\lambda = 2$ and a fixed step size $\mu = 0.005$. Spatially diffuse white noise is added at a SNR of 10 dB.

To illustrate the efficiency of the algorithm proposed in Section III-A2), we first considered in Fig. 4(a) the case of four plane-wave narrowband and uncorrelated moving sources with a unit power emitting from separate initial angles. Simulation results show that the algorithm applying Section III-A2) has a better performance than the algorithm based on adaptive beamformers presented in Section III-A1) regarding beamforming and tracking behavior. This improved performance is due to the fact that adaptive beamformers introduce an extra misadjustment.

Fig. 4(c) shows that the output signal distortion converges to optimal performance in source signal extraction 22 dB ($10\log_{10}(16)$ + SNR; see [1]–[3]). Fig. 4(d) shows that the mean interference in source separation over all estimated signals $\sum_{i=1}^{p}\sum_{j=1,j\neq i}^{p} \|W_{j,t}^H G_{i,t}\|^2/p$ is efficiently reduced down to -33 dB. Moreover, the time constant in Fig. 4(b) corresponds practically to $\frac{1}{\mu\sigma_{s_i}^2}$. However, we see in Fig. 4(b)–(d) that the tracking and the source signal extraction are disturbed when two of the targets are either too close or cross.

To illustrate the performance of the speed estimation procedure, we considered the case of two crossing targets with uniform speeds as shown in Fig. 5(a). Without the speed estimation procedure, both trackers produce an estimation delay and turn back at the crossover point. Although both sources remain tracked, the result is not satisfactory:

- The estimated tracks have a bias of 2° (see Fig. 5(a) and (b)).
- The mean signal distortion in source extraction converges to 19 dB (3 dB loss in SNR).
- Regarding the classification of the targets, the estimated tracks are permuted after the crossover (see Fig. 5(a) and (b)).

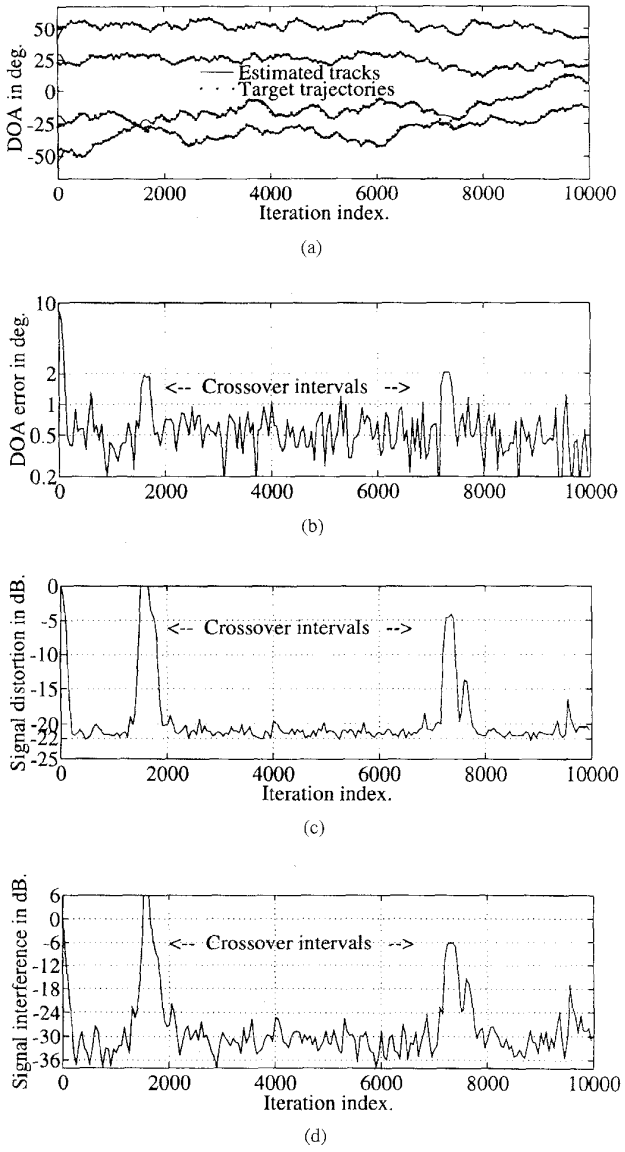

Fig. 4. (a) DOA trajectories and estimated tracks of four sources; (b) mean of localization errors $\sum_{i=1}^{p} |\hat{\phi}_{i,t} - \phi_{i,t}|/p$; (c) mean of signal distortion $\sum_{i=1}^{p} |\hat{s}_{i,t} - s_{i,t}|^2/p$; (d) mean of the interference in source separation $\sum_{i=1}^{p} \sum_{j=1,j\neq i}^{p} ||W_{j,t}^H G_{i,t}||^2/p$.

On the other hand, the speed estimation procedure removes the bias and maintains the tracking during and after the crossover, where the values of ϵ in (12) and α in (10) are experimentally chosen, respectively, equal to 0.08 and 0.01. Fig. 5(b) and (c), respectively, show 34 dB improvement in source localization and 3 dB enhancement in beamforming (optimal output SNR). Of course, when the targets are too close around the crossover point, the sources are confused and cannot be separated. Fig. 5(d) and (e) show that the speeds are estimated with a very small error of about $10^{-4\circ}$/sample. We also notice, in Fig. 5(b), (d), and (e), the second order nature of the global algorithm in tracking where the corresponding time constants belong to $[\frac{1}{\mu\sigma_s^2}, \frac{2}{\mu\sigma_s^2}]$. We finally notice a better capability of the algorithm to cancel fast mobile jammers in

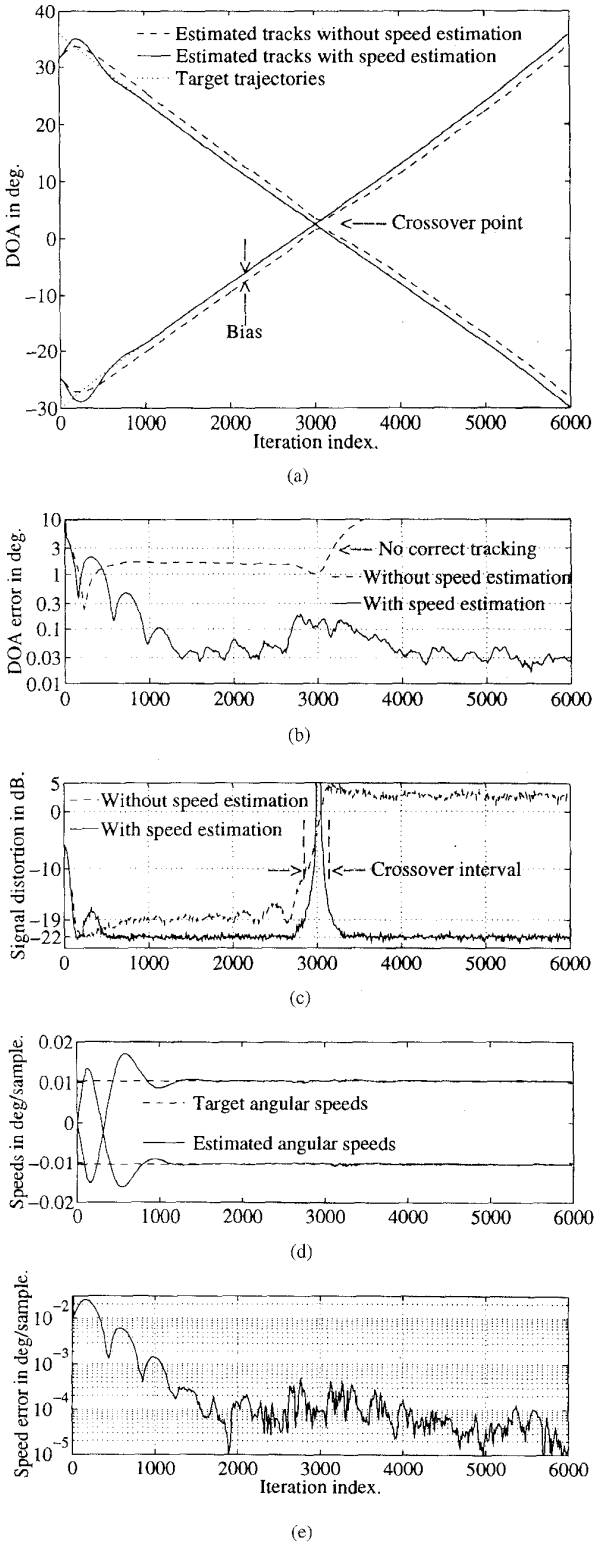

Fig. 5. (a) DOA trajectories and estimated tracks of two crossing sources (linearly moving targets; first-order crossover) with and without speed estimation; (b) performance of target tracking, mean of localization errors $\sum_{i=1}^{p} |\hat{\phi}_{i,t} - \phi_{i,t}|/p$; (c) performance of source separation, mean of total distortion $\sum_{i=1}^{p} E[|\hat{s}_{i,t} - s_{i,t}|^2]/p$; (d) speed estimation (in degree per sample); (e) mean absolute error of estimated speeds $\sum_{i=1}^{p} |\frac{180}{2\pi^2}(\hat{\kappa}_{i,t} - \kappa_{i,t})|/p$ (in degrees per sample).

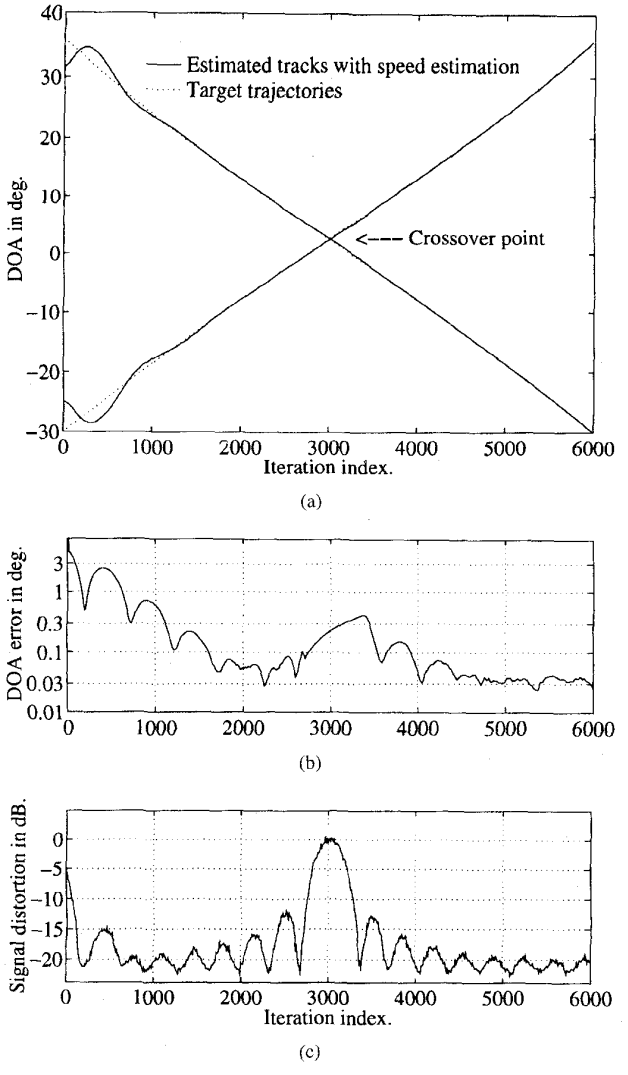

Fig. 6. Adaptive normalized LMS beamformers with GSC structure: (a) DOA trajectories and estimated tracks of two crossing sources (linearly moving targets; first-order crossover) with speed estimation; (b) performance of target tracking, mean of localization errors $\sum_{i=1}^{p} |\hat{\phi}_{i,t} - \phi_{i,t}|/p$; (c) performance of source separation, mean of total distortion $\sum_{i=1}^{p} E[|\hat{s}_{i,t} - s_{i,t}|^2]/p$.

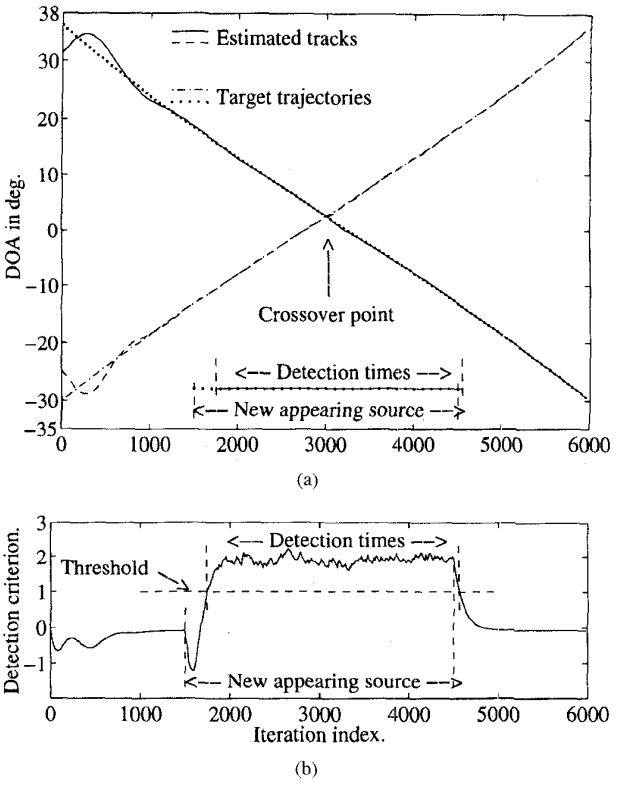

Fig. 7. Detection and initialization of a new appearing source at $t = 1500$ and detection of its disappearance at $t = 4500$. (a) Trajestories and estimated tracks. (b) Energy-based detection curve.

comparison with adaptive beamformers like the GSC structure [22] in Fig. 6.

To illustrate the performance of source number tracking, in Fig. 7, we added a third source appearing at $t = 1500$ and vanishing at $t = 4500$ with the same scenario ($\sigma_{s_3}^2 = 2$, $a = \mu_d = 0.01$). This source is effectively detected after a time delay that corresponds to the sum of the initial localization delay τ_{init} in (15) and the energy estimation delay $\tau_{e_{p+1}}$ in (16). On the other hand, its extinction is detected with a time delay equal to $\tau_{e_3} = \frac{0.6}{a} = 60$.

In Fig. 8(a), we considered two targets that have equal speeds during crossover. The tracking in this case is made possible using the estimation of the second-order increments (see [2] and [3]). Fig. 8(b) confirms the intuitive expectation regarding the tracking of third-order crossovers using the estimation of the third-order increments. In all experiments, we saw that the estimation of higher order increments does not improve the tracking behavior except during complex crossovers.

In Fig. 9, we considered two zero mean source signals with variances equal to 1 and a correlation factor equal to $\rho = 0.9$. The sources are immobile at 40° and 70°. DOA's are initialized with a 8° error. Although the partial coherence between the sources could produce a bias and/or an extra time constant in tracking, Fig. 9(a) and (b) shows that the algorithm is capable of tracking the partially coherent sources with a same order of localization error as the incoherent sources. We observe in Fig. 9(c) that the algorithm is not robust to coherent interference with the adaptive beamformers, whereas it avoids the signal cancelation with conventional beamformers. In this case, the output signal distortion converges to the optimal value −22 dB. Finally, further tests successfully made with full coherent sources were recently described in [3].

VI. Conclusion

We presented, in this paper, a new algorithm for robust multisource beamforming and multitarget tracking. First, we described the generalization made of the work recently presented in the single source case. It should be noted here that adaptive beamformers such as the GSC could be used to extract the desired source signals with optimal reduction of spatially correlated noise when no coherent interference is present. Given the assumption that the number and the approximate initial locations of the most significant sources are

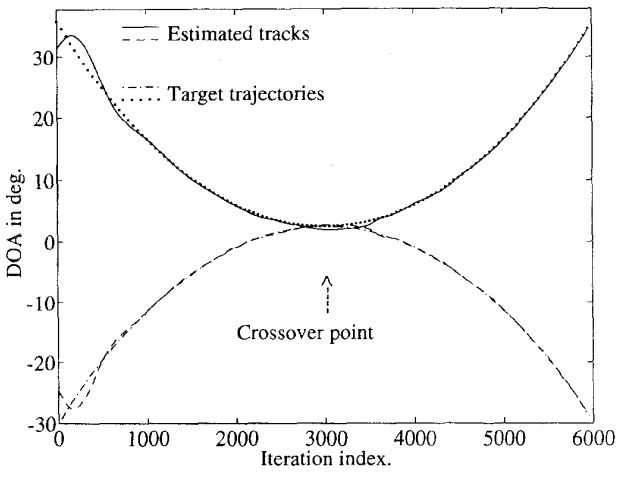

(a)

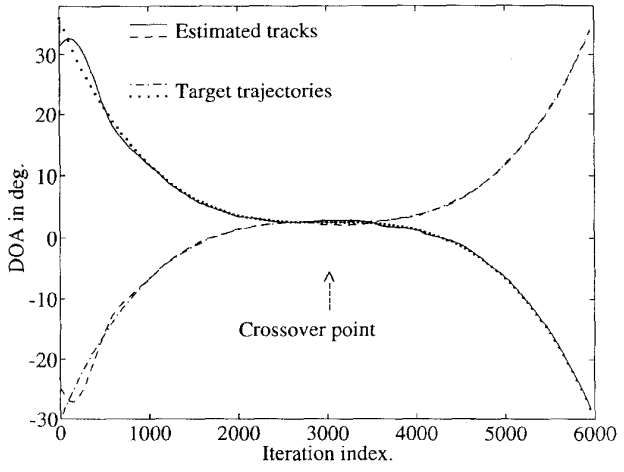

(b)

Fig. 8. Target tracking with the estimation of higher order increments for complex crossovers. (a) Second-order crossover. (b) Third-order crossover.

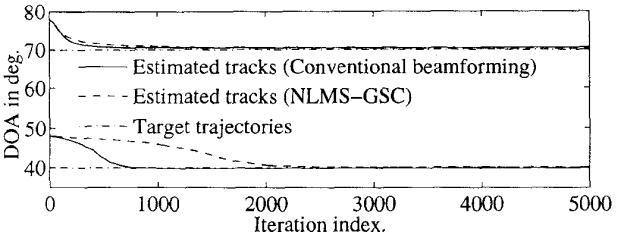

(a)

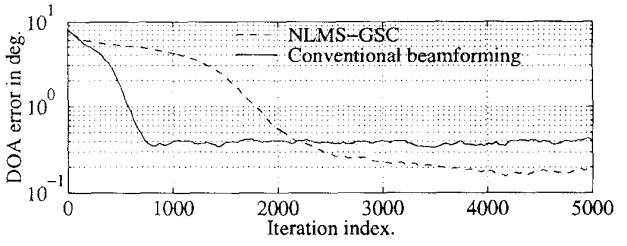

(b)

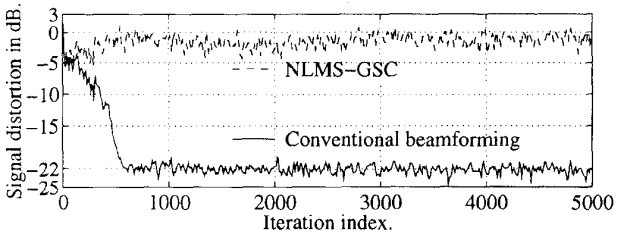

(c)

Fig. 9. (a) DOA trajectories and estimated tracks of two coherent immobile sources. (b) Mean of localization errors $\sum_{i=1}^{p} |\hat{\phi}_{i,t} - \phi_{i,t}|/p$. (c) Mean of signal distortion $\sum_{i=1}^{p} |\hat{s}_{i,t} - s_{i,t}|^2/p$.

known (the sources may be adaptively detected and initialized by a marginal proposed procedure), we proved that the use of conventional beamformers is optimal in the presence of uncorrelated white noise and correlated sources. The beamforming algorithm has the same robustness with regard to location errors. We also showed that the resulting localization algorithm offers the same asymptotic localization performance as the MUSIC algorithm for immobile targets. On the other hand, it is highly advantageous for mobile and maneuvering sources (see also [1]).

Particularly in the case where the time increment of a location parameter is not zero mean, the location estimate is biased. Hence, we proposed a new procedure based on the use of certain estimated kinematic parameters (e.g., the speed), which is proved to yield unbiased estimates. Simultaneously, the estimated kinematic parameters are shown to solve some of the problems of crossing targets via the prediction of their trajectories. Although the signal separation is not possible for the targets during their crossover, the target tracking is made possible by the *a priori* information collected on the kinematics of their trajectories (i.e., speed, acceleration, etc.).

All the steps of the algorithm involve a computational complexity of order $O(mp)$, where p and m are, respectively, the number of sources and array sensors (except $O(mp^2 + mp + p^3 + p^2)$ when using (4)). Hence, it can be implemented quite easily. Finally, further results regarding complexity reduction and an optimal structure for coherent source extraction in correlated noise were recently given among other generalizations [3], [24], [2].

Appendix A
Iterative Equation of Localization Error

For convergence analysis, we consider the case of a single source and white noise, where $R_N = \sigma_N^2 I$. The origin is defined at the array center (i.e., $\sum_{q=1}^{m} x_q = 0$). As in [2] and [3], we can see that

$$\Delta\tilde{\kappa}_{i,t} = (1 - r_{i,t})\Delta\hat{\kappa}_{i,t-1} + u_{i,t} \tag{27}$$

where

$$r_{i,t} \triangleq \mu\left(s_{i,t}s_{i,t}^H + \mathrm{Re}\left\{ s_{i,t}N_t^H \frac{F(\hat{\kappa}_{i,t-1})}{m} \right\} \right),$$

$$u_{i,t} \triangleq \frac{\mu}{\sum_{q=1}^{m} x_q^2}\mathrm{Re}\left\{F^H(\hat{\kappa}_{i,t-1})DN_tN_t^H\frac{F(\hat{\kappa}_{i,t-1})}{m}\right\} + \frac{\mu}{\sum_{q=1}^{m} x_q^2}\mathrm{Re}\left\{F^H(\hat{\kappa}_{i,t-1})DN_ts_{i,t}^H\right\},$$
$$D \triangleq \mathrm{diag}[jx_q]$$

where $\mathrm{Re}\{\cdot\}$ denotes the real part of a complex number. To proceed, we first replace (11) in (27). The result of (27) is then replaced in (10). By the definition of $\psi_{i,t}$ in (20), we may rewrite the results of (27)) and (10) in matrix form. Thus, we obtain (21)

$$\psi_{i,t} = \begin{bmatrix} 1-r_{i,t} & 1-r_{i,t} \\ \alpha r_{i,t} & 1+\alpha r_{i,t} \end{bmatrix}\psi_{i,t-1} + \begin{bmatrix} u_{i,t} \\ \alpha u_{i,t} + \ddot{\kappa}_{i,t} \end{bmatrix}$$

where $\ddot{\kappa}_{i,t} \triangleq 2\kappa_{i,t-1} - \kappa_{i,t} - \kappa_{i,t-2}$ is the target angular acceleration.

Appendix B
Iterative Equation for the Covariance of Localization Error

In this Appendix, the covariance of $\psi_{i,t}$ in (21) is computed. Using (27), we have

$$E[\Delta\tilde{\kappa}_{i,t}\Delta\tilde{\kappa}_{i,t-1}] \triangleq (1-\mu\sigma_{s_i}^2)(E[|\Delta\tilde{\kappa}_{i,t-1}|^2] + E[\Delta\tilde{\kappa}_{i,t-1}\Delta\dot{\kappa}_{i,t-1}]) \quad (28)$$

$$E[\Delta\tilde{\kappa}_{i,t}\Delta\dot{\kappa}_{i,t-1}] \triangleq (1-\mu\sigma_{s_i}^2)(E[|\Delta\dot{\kappa}_{i,t-1}|^2] + E[\Delta\tilde{\kappa}_{i,t-1}\Delta\dot{\kappa}_{i,t-1}]). \quad (29)$$

By (27), we can show as in [2] and [3] that

$$E[|\Delta\tilde{\kappa}_{i,t}|^2] = P_iE[|\Delta\hat{\kappa}_{i,t}|^2] + Q_i \quad (30)$$

where

$$P_i \triangleq 1 - 2\mu\sigma_{s_i}^2 + \mu^2\left(2\sigma_{s_i}^4 + \frac{\sigma_{s_i}^2\sigma_N^2}{2m}\right) \quad (31)$$

$$Q_i \triangleq \frac{\mu^2\sigma_N^2(\sigma_N^2 + m\sigma_{s_i}^2)}{2m\sum_{q=1}^{m} x_q^2}. \quad (32)$$

By (11) and (10), we, respectively, obtain

$$E[|\Delta\tilde{\kappa}_{i,t}|^2] = P_i\{E[|\Delta\tilde{\kappa}_{i,t-1}|^2] + E[|\Delta\dot{\kappa}_{i,t-1}|^2] + 2E[\Delta\tilde{\kappa}_{i,t-1}\Delta\dot{\kappa}_{i,t-1}]\} + Q_i \quad (33)$$

$$E[|\Delta\dot{\kappa}_{i,t}|^2] = (1-\alpha)^2E[|\Delta\dot{\kappa}_{i,t-1}|^2] + \alpha^2E[|\Delta\tilde{\kappa}_{i,t} - \Delta\tilde{\kappa}_{i,t-1}|^2] + \sigma_{\ddot{\kappa}}^2 + 2\alpha(1-\alpha)E[\Delta\dot{\kappa}_{i,t-1}(\Delta\tilde{\kappa}_{i,t} - \Delta\tilde{\kappa}_{i,t-1})] \quad (34)$$

where $\sigma_{\ddot{\kappa}}^2 = E[\ddot{\kappa}_t^2]$, and

$$E[\Delta\tilde{\kappa}_{i,t}\Delta\dot{\kappa}_{i,t}] = (1-\alpha)E[\Delta\dot{\kappa}_{i,t-1}\Delta\tilde{\kappa}_{i,t}] + \alpha(E[|\Delta\tilde{\kappa}_{i,t}|^2] - E[\Delta\tilde{\kappa}_{i,t}\Delta\tilde{\kappa}_{i,t-1}]). \quad (35)$$

Defining $\Psi_{i,t} = [E[|\Delta\tilde{\kappa}_{i,t}|^2], E[|\Delta\dot{\kappa}_{i,t}|^2], E[\Delta\tilde{\kappa}_{i,t}\Delta\dot{\kappa}_{i,t}]]^T$ and rewriting the results of this Appendix given by (28)–(35) in a matrix form, we obtain

$$\Psi_{i,t} = \Sigma_i\Psi_{i,t-1} + \Re_i \quad (36)$$

where

$$\Sigma_i = P_i\begin{bmatrix} 1 & 1 & 2 \\ \alpha^2 & \alpha^2 & 2\alpha^2 \\ \alpha & \alpha & 2\alpha \end{bmatrix} + \left(1-\mu\sigma_{s_i}^2\right)\begin{bmatrix} 0 & 0 & 0 \\ -2\alpha^2 & 2\alpha(1-\alpha) & 2\alpha(1-2\alpha) \\ -\alpha & (1-\alpha) & (1-2\alpha) \end{bmatrix} + \begin{bmatrix} 0 & 0 & 0 \\ \alpha^2 & (1-\alpha)^2 & -2\alpha(1-2\alpha) \\ 0 & 0 & 0 \end{bmatrix} \quad (37)$$

$$\Re_i = \left[Q_i, \sigma_{\ddot{\kappa}}^2 + \alpha^2Q_i, \alpha Q_i\right]^T. \quad (38)$$

References

[1] S. Gazor, S. Affes, and Y. Grenier, "Robust adaptive beamforming via target tracking," *IEEE Trans. Signal Processing*, vol. 44, 1996.

[2] S. Gazor, "Optimization d'une antenne acoustique pour la prise de son," Ph.D. dissertation, Ecole Nationale Supérieure des Télécommunications, Paris, France, Nov. 1994.

[3] S. Affes, "Formation de voie adaptative en milieux réverbérants," Ph.D. dissertation, Ecole Nationale Supérieure des Télécommunications, Paris, France, Oct. 1995.

[4] S. Gazor, S. Affes, and Y. Grenier, "Robust multi-source beamforming via LMS-like target tracking," in *Proc. EURASIP EUSIPCO'94*, Edinburgh, U.K., vol. I, Sept. 13–16, 1994, pp. 339–342.

[5] L. J. Griffiths and C. W. Jim, "An alternative approach to linearly constrained adaptive beamforming," *IEEE Trans. Antennas Propagat.*, vol. AP-30, pp. 27–34, Jan. 1982.

[6] Y. Bar-Shalom and T. E. Fortmann, *Tracking and Data Association*. New York: Academic, 1988.

[7] N. W. Whinnett and A. Manikas, "High-resolution array processing methods for joint direction-velocity estimation," *Proc. Inst. Elec. Eng.*, pt. F, vol. 140, no. 2, pp. 114–122, Apr. 1993.

[8] Y. Bar-Shalom, *Multitarget-Multisensor Tracking: Advanced Applications*. Boston, MA: Artech House, 1990.

[9] S. C. Nardone, A. G. Lindgren, and K. F. Gong, "Fundamental properties and performance of conventional bearings-only target motion analysis," *IEEE Trans. Automat. Contr.*, vol. AC-29, pp. 775–787, Sept. 1984.

[10] C. R. Rao, L. Zhang, and L. C. Zhao, "Multiple target angle tracking using sensor array outputs," *IEEE Trans. Aerospace Electron. Syst.*, vol. 29, pp. 268–271, Jan. 1993.

[11] ——, "Multitarget angle tracking algorithm for data association," *IEEE Trans. Signal Processing*, vol. 42, pp. 459–462, Feb. 1994.

[12] C. K. Sword, M. Samaan, and E. W. Kamen, "Multiple target angle tracking using sensor array outputs," *IEEE Trans. Aerospace Electron. Syst.*, vol. 26, pp. 367–373, Mar. 1990.

[13] W. K. Lo and K. C. Li, "An improved multiple target angle tracking algorithm," *IEEE Trans. Aerospace Electron. Syst.*, vol. 28, pp. 797–805, July 1992.

[14] S. B. Park, C. S. Ryu, and K. K. Lee, "Multiple target angle tracking algorithm using predicted angles," *IEEE Trans. Aerospace Electron. Syst.*, vol. 30, pp. 643–648, Apr. 1994.

[15] P. A. Thompson, "An adaptive spectral analysis technique for unbiased frequency estimation in the presence of white noise," in *Proc. 13th Asilomar Conf. Circuits, Syst. Comput.*, Nov. 1980, pp. 529–533.

[16] E. Oja, "A simplified neuron model as a principal component analyzer," *J. Math. Biol.*, vol. 15, pp. 267–273, 1982.

[17] B. Yang, "Subspace tracking based on the projection approach and the recursive least squares method," in *Proc. IEEE ICASSP'93*, Minneapolis, Apr. 27–30, 1993, vol. IV, pp. 145–148.

[18] A. Eriksson, P. Stoica, and T. Söderström, "On-line subspace algorithms for tracking moving sources," *IEEE Trans. Signal Processing*, vol. 42, no. 9, pp. 2319–2330, Sept. 1994.

[19] P. Stoica and A. Nehorai, "MUSIC, maximum likelihood and Cramer–Rao bound," *IEEE Trans. Acoustics, Speech, Signal Processing*, vol. 37, pp. 720–741, May 1989.
[20] J. J. Fuchs, "Estimation of the number of signals in the presence of unknown correlated sensor noise," *IEEE Trans. Signal Processing*, vol. 40, pp. 1053–1061, May 1992.
[21] Q. T. Zhang and K. M. Wong, "Information theoretic criteria for the determination of the number of signals in spatially correlated noise," *IEEE Trans. Signal Processing*, vol. 41, pp. 1652–1663, Apr. 1993.
[22] S. Haykin, *Adaptive Filter Theory*. Englewood Cliffs, NJ: Prentice-Hall, 1991, 2nd ed.
[23] R. W. Hamming, *Digital Filters*, 3rd ed. Englewood Cliffs, NJ: Prentice-Hall, 1989.
[24] S. Gazor, S. Affes, and Y. Grenier, "Wideband multi-source beamforming with adaptive array location calibration and direction finding," in *Proc. IEEE ICASSP'95*, Detroit, MI, vol. III, pp. 1904–1907.

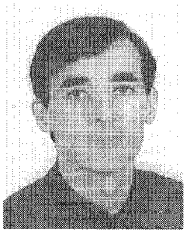

Sofiène Affes was born in Kasserine, Tunisia, on September 19, 1969. He received the Ingénieur degree in electrical engineering in 1992 and the Ph.D. degree in the field of signal and image processing in 1995, both from Ecole Nationale Supérieure des Télécommunications, Paris, France.

During 1991, he was a junior visitor at the Cambridge University Engineering Department, Cambridge, U.K., working on speech recognition. He is currently a Post-Doctoral fellow at the Institut National de la Recherche Scientifique-Télécommunications, Montreal, Canada, working on personal communication systems. His interests are in signal and array processing, with applications to acoustics and speech processing, and digital communications. He has been involved in European ESPRIT projects (2101 ARS during 1991 and 6166 FREETEL from 1993 to 1994).

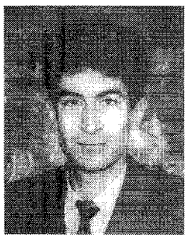

Saeed Gazor was born in Isfahan, Iran, on December 12, 1964. He received the B.Sc. degree in electrical engineering in 1987 and the M.Sc. degree in communication engineering in 1989, both from Isfahan University of Technology, Isfahan, Iran, and the Ph.D. degree in the field of signal and image processing from Ecole Nationale Supérieure des Télécommunications, Paris, France, in 1994.

From 1989 to 1990, he was with the Iran Air Force doing his national service. His interests are in mathematics, adaptive signal processing, and array signal processing (with applications to source tracking, beamforming, and echo cancellation).

Yves Grenier (A'80–M'81) was born in Ham, Somme, France, in 1950. He received the Ingénieur degree from Ecole Centrale de Paris in 1972, the Docteur-Ingénieur degree from Ecole Nationale Supérieure des Télécommunications, Paris, in 1977, and the Doctorat d'Etat es Sciences Physiques from the University of Paris-Sud in 1984.

Since 1977, he has been with Ecole Nationale Supérieure des Télécommunications, Paris, as an Assistant and, since 1984, as Professor. Until 1977, his interests were in speech recognition, speaker identification, and speaker adaptation of recognition systems. Since then, he has been working on signal modeling, spectral analysis of noisy signals with applications in speech recognition and synthesis, estimation of nonstationary models, and time–frequency representations. He is presently interested in array processing with applications to acoustics (acoustic echo cancellation, noise reduction, and microphone arrays). He coorganized a SFA (previously GALF) workshop on speech signal analysis in Paris in December 1983 and organized a CNRS seminar on nonstationary modeling in Nice, France, in June 1984.

Dr. Grenier was the Editor of a special issue of *Signal Processing* on Major Trends in Spectral Analysis (vol. 10, no. 1, 1986). He is a member of SFA (Société Française d'Acoustique). He has been involved in European ESPRIT projects (2101 ARS from 1989 to 1992 and 6166 FREETEL from 1992 to 1994).